

Quantum dot coupled to unconventional superconducting electrodes *

Yshai Avishai^{1,2,*}, Tomosuke Aono¹, and Anatoly Golub¹

¹*Department of Physics and ²Ilse Katz Center for Nanotechnology,
Ben-Gurion University, Beer-Sheva 84105, Israel*

**Corresponding author: yshai@bgumail.bgu.ac.il*

Received 13 November 2003

Abstract

While Quantum dots connected on both sides to *normal* metallic leads is a central research topic in contemporary condensed matter physics, there is now a growing interest in the question of what happens if one or both leads are *superconducting*. In a series of papers we have developed a theoretical basis for the relevant physical situation. As it turns out, the resulting physical observables strongly depend on the symmetry of the superconducting electrodes order parameter. previously, we have studied the case of *s*-wave superconducting electrodes. Here, in this work, the physics of junctions containing *p*-wave superconducting and normal leads weakly coupled to an Anderson impurity in the Kondo regime is elucidated. For *unconventional* (unlike *s* wave) superconducting leads, mid-gap surface states play an important role in the tunneling process and help the formation of the Kondo resonance. The current, shot-noise power and Fano factor are calculated and displayed as functions of the applied voltage V in the sub-gap region $eV < \Delta$ (the superconducting gap). In addition, the Josephson current for a quantum dot in the Kondo regime weakly coupled on both sides to *p*-wave superconductors is computed as function of temperature and phase. The peculiar differences between the cases of *s*-wave and *p*-wave superconducting leads are pointed out.

PACS: 74.70.Kn, 72.15.Gd, 71.10.Hf, 74.20.Mn

*Presented at International Workshop *Frontiers in Science and Technology*.
Holon Academic Institute of Technology, Holon, Israel, 26-27 October 2003

1 Introduction

This research focuses on transport through an interacting quantum dot in the Kondo regime weakly coupled to p -wave superconducting leads [1]. It is quite conceivable that the role of the quantum dot can be played also by a single molecule or by a Carbon nano-tube. Recently, it has been unambiguously established that the Kondo physics [2] plays an important role in electron transport through quantum dots, where instead of a magnetic impurity one encounters localized electrons [3 - 5]. Observations of the Kondo effect in transport through quantum dots [6, 7], in carbon nano-tubes (*CNT*) [8], in vertical dots [9], and in single molecules [10] demonstrate the feasibility of exploiting tunable physical parameters in these systems in order to yield important information on the Kondo physics and other many-body related phenomena.

The Kondo physics in a quantum dot attached on both its sides to *normal* metallic leads received much recent attention. Many experiments and theoretical investigations are devoted to its study ever since the first experiments were reported in 1998. Recently, it has been realized that novel physical effects emerge if (one or both) electrodes is a superconductor [11]. Hereafter we abbreviate by N a normal metallic lead, by S a superconducting lead and by K a quantum dot in the Kondo regime weakly attached to N and/or S leads. SKS and SKN junctions can now be fabricated in laboratories. Moreover, there are also natural candidates: Fabrication of superconducting junctions with a weak link formed by *CNT* have already been reported [12, 13].

In a series of recent works [14, 15] we have developed a formalism for the study of transport in SKN and SKS junctions. It is then useful to state clearly at this point the peculiar aspects of the present work compared with the previous ones. In Ref. [14] the underlying physics of SKS and SKN junctions was analyzed out of the Kondo regime, that is, at $\Delta \gg T_K$ (the Kondo temperature), while in Ref. [15] attention is focused on SKS junctions for which the leads are composed of s -wave superconductors. Here we are particularly interested in electron transport in the Kondo regime in SKN junctions for which the S lead is composed of a p -wave superconductor. The physics of junctions with p -wave superconducting leads is essentially distinct from that pertaining to junctions with s -wave superconducting leads (especially in the Kondo regime) as is carefully explained and underlined below. Thus, while we heavily rely on the computational machinery developed earlier, the results obtained here are novel.

One of the crucial differences between the case of normal and supercon-

ducting leads touches upon the question of how electrons are transported from one lead to the other. The central electron-transport mechanism in *SKS* and *SKN* junctions is that of Andreev reflections when two particles tunnel together coherently to form a Cooper pair in the superconductor. Of course, Andreev reflections play an important role in bulk *SIS* and *SN* junctions (here *I* denotes an insulating layer). In the former case they are responsible for occurrence of direct Josephson current while in the latter case they enhance the conductance by a factor 2.

What is the role of Andreev reflections in quantum dots such as *SKS* and *SKN* junctions? The answer to this question is rather interesting and exposes a subtle distinction between the cases of *s*-wave and *p*-wave superconductors. The pertinent physics is governed by the interplay of Andreev reflections and the formation of the Kondo-resonance in the spectral density of states of the dot electron [11]. In the case of an *SKN* junction when one electrode is an *s*-wave superconductor and the Kondo impurity is weakly coupled to the *S* and *N* electrodes, the physics is determined by competition between two phenomena. The first one is the formation of a Kondo singlet which screens the bare impurity spin and drives the system toward the unitary limit at very low temperatures. The second one is the existence of the superconducting gap which implies a vanishingly small density of low energy electron states [16 - 18]. These are precisely the electron states which are needed in order to screen the Kondo impurity. A relevant parameter in this context is the ratio between the Kondo temperature and the superconducting gap,

$$t_K \equiv \frac{T_K}{\Delta}. \quad (1)$$

When $t_K < 1$, the Kondo effect is suppressed by the superconducting gap while for $t_K > 1$, the Kondo effect (close to the unitary limit) and superconductivity coexist. Indeed, for $t_K > 1$, electron states outside the gap can participate in the screening interaction. Several works have studied these aspects both for $t_K < 1$ [18, 16], and for $t_K > 1$ [17, 15, 19, 20]. In a recent experiment [13], a crossover around $t_K = 1$ has been realized in *SKS* junctions.

Consider, on the other hand, an *SKN* junction in which the *S* electrode consists of an *unconventional* superconductor. To be more specific, we mean superconductors with triplet pairing, such that the order parameter has a *p*-wave orbital symmetry. Such *p*-wave superconductors have recently been discovered by Maeno *et al* [1] in *Sr₂RuO₄*. The fact that in these superconductor the order parameter is not rotationally symmetric implies a special

importance for its orientation when it is integrated into a junction. In particular, let us assume that the superconductor is oriented relative to the interface in such a way that the pair potential reverses its sign on the Fermi surface. In this case, zero-energy states (*ZES*) are formed (that is, *inside the gap*), which are localized near the surface of the unconventional superconductor. These states can now participate in screening the impurity spin through the Kondo effect and emergence of sub-gap current is expected. For example, in the experimentally feasible setup of $S - CNT - N$ where just a few tunneling channels are present, charge is carried mainly by quasiparticles moving perpendicular to the interface. This restricts the possible values of the angle θ between the superconducting surface and the direction of the injected quasiparticles [21]. Formation of *ZES* is possible when $\Delta(\theta) = -\Delta(\pi - \theta)$. If the impurity is almost point-like, the relevant injection angle is of course $\theta = 0$. For impurities of finite extent, one may also consider formation of *ZES* in *d*-wave superconductors. Thus, the physics of *SKN* junctions with an *S* electrode whose order parameter has a non-trivial symmetry is affected by the formation of *ZES* in the Kondo regime. In short, the physics of *SKN* junction will be prominently different between *s*-wave on the one hand and *p* or *d*-wave superconductors on the other hand.

The question now arises is whether the above mentioned distinction between the cases of *s*-wave and *p*-wave superconducting electrodes can be elucidated. We answer it positively by calculating a number of transport observables in *SKN* junctions for several values of t_K . Beyond investigating the conductance dependence on the applied bias we also explore the shot-noise and the Fano factor. Moreover, at zero bias we also consider *SKS* junctions and analyze the Josephson (direct) current dependence on the phase difference between the two superconductors as well as on the temperature. In Section 2 the model Hamiltonian is written in terms of the slave boson formalism. The Green functions pertaining to *p* wave superconducting leads are introduced and the mean-field slave boson approximation (MFSBA) is briefly discussed. Calculations and presentations of conductance, shot-noise power and Josephson current are respectively detailed in Sections 3, 4 and 5.

2 Model Hamiltonian and *p* wave Green functions

The formalism employed below is the slave boson mean-field approximation, explained and justified in our earlier works [14, 15]. Therefore we will skip most of it except the definitions of Green functions peculiar for the case

of p -wave superconducting lead. The model Hamiltonian of SKN or SKS junctions is represented by the Anderson model with the superconducting lead:

$$H = H_L + H_R + H_d + H_t + H_c, \quad (2)$$

in which H_j ($j = L, R$) are the Hamiltonians of the electrodes which depend on the electron field operators $\psi_{a\sigma}(\mathbf{r}, t)$ at $\mathbf{r} = (x, y)$ with the spin $\sigma = \pm$. For a superconducting lead we have,

$$H_j = \sum_{j=L,R} \int_j dr \left(\psi_{j,+}^\dagger(r) \psi_{j,-}(r) \right) \begin{pmatrix} \xi(\nabla) & \Delta_j \\ \Delta_j^* & -\xi(\nabla) \end{pmatrix} \begin{pmatrix} \psi_{j,+}(r) \\ \psi_{j,-}(r) \end{pmatrix}, \quad (3)$$

where $\xi(\nabla) = -\nabla^2/2m - \mu$ with the chemical potential μ depends on the bias voltage V , and Δ is the Cooper pairing potential. For s -wave superconductor, Δ is isotropic (in fact it is a constant) while for p -wave superconductor, Δ is anisotropic and depends on the two dimensional momentum vector: $\Delta(\alpha) = |\Delta|(k_x + ik_y)/|k| = |\Delta|\exp(i\alpha)$ with the azimuthal angle $\alpha = \arctan(k_y/k_x)$. This pairing potential changes the sign: $\Delta(\alpha) = -\Delta(\pi - \alpha)$. For a normal lead, $\Delta = 0$ of course.

The quantum dot consists of a single energy level $\epsilon_0 < 0$ with Coulomb interaction U . We assume that $U \rightarrow \infty$ to exclude double occupancy of electrons in the dot. In this scheme, the annihilation operator d_σ of electron in the dot is written as $d_\sigma = b^\dagger c_\sigma$ with the slave boson operator b and the pseudo fermion operator c_σ and the constraint term of H_c :

$$H_c = \lambda \left(\sum_\sigma c_\sigma^\dagger c_\sigma + b^\dagger b - 1 \right), \quad (4)$$

where λ is a Lagrange multiplier [22]. The corresponding dot and tunneling Hamiltonians, H_d and H_t are expressed as:

$$\begin{aligned} H_d &= \epsilon_0 \sum_\sigma c_\sigma^\dagger c_\sigma, \\ H_t &= \sum_{j\sigma} \mathcal{T}_j c_\sigma^\dagger b \psi_{j\sigma}(\mathbf{0}, t) + h.c., \end{aligned} \quad (5)$$

where \mathcal{T}_j is the tunneling amplitude. If the quantum dot is almost point-like, the relevant value of α for the pairing potential is zero.

Since electron field in the dot couples only with $\psi_{j\sigma}(\mathbf{0}, t)$, (referred to as *surface states*), we can integrate out electron fields inside the lead [14].

Following Ref. [15] let us consider the dynamical “partition function”

$$Z \sim \int \mathcal{D}[F] \exp(i\mathcal{S}), \quad (6)$$

where the path integral is carried out over all fields $[F]$ and the action \mathcal{S} is obtained by integrating the Lagrangian pertaining to the Hamiltonian (2) along the Keldysh contour. In performing the functional integrations the boson field operators are treated as c -numbers. As a result one arrives at an effective action expressed in terms of the Green functions of the leads.

$$S_{\text{eff}} = -i\text{Tr} \ln \hat{G}^{-1} - \int dt [\hat{\lambda} \sigma_z (\hat{b}\hat{b} - 1)]. \quad (7)$$

Here $\hat{\lambda} = (\lambda_1, \lambda_2)$, $\hat{b} = (b_1, b_2)$ and σ_z are diagonal matrices acting in Keldysh space. The inverse propagator \hat{G}^{-1} depends on the Green functions of the electrodes [14]. Performing the standard basis rotation in Keldysh space one finds,

$$\hat{G}^{-1}(\epsilon, \epsilon') = \delta(\epsilon - \epsilon') (\epsilon - \tau_z \tilde{\epsilon} - \frac{\Gamma b^2}{2} \tau_z \hat{g}_+(\epsilon) \tau_z), \quad (8)$$

where $\tilde{\epsilon} = \epsilon_0 + \lambda$ is the renormalized level position (in the Kondo limit one has $\tilde{\epsilon} \simeq 0$) and $\Gamma = (\Gamma_L + \Gamma_R)/2 \propto \mathcal{T}_{\mathcal{L},\mathcal{R}}^2$ is the usual transparency parameter. The 2×2 matrix representation (in Keldysh space) for g is composed of diagonal elements $\hat{g}^{R/A}(\epsilon)$ and an upper off-diagonal element $\hat{g}^K(\epsilon) = (\hat{g}^R - \hat{g}^A) \tanh(\epsilon/2T)$. Here and below we define

$$\hat{g}_{\pm} = \gamma_L \hat{g}_L \pm \gamma_R \hat{g}_R, \quad (9)$$

with asymmetry parameters $\gamma_j = \Gamma_j/\Gamma$. The matrix \hat{g}_R has the standard structure with retarded and advanced superconductor Green functions which in the s -wave case reads,

$$\hat{g}^{R/A}(\epsilon) = i \frac{(\epsilon \pm i0) + |\Delta| \tau_x}{\sqrt{(\epsilon \pm i0)^2 - |\Delta|^2}}, \quad (10)$$

The retarded and advanced Green functions $g^{R/A}(\epsilon)$ for the surface states of the p -wave superconductor with incident angle α is represented by 2×2 matrices:

$$\hat{g}^{R/A}(\epsilon) = \hat{g}_1^{R/A} \mathbf{1} + \hat{g}_2^{R/A} \tau_x, \quad (11)$$

with

$$\begin{aligned}\hat{g}_1^{R/A} &= \frac{i\sqrt{(\epsilon \pm 0)^2 - |\Delta|^2} \cos \alpha - \epsilon \sin \alpha}{\epsilon \cos \alpha + i\sqrt{(\epsilon \pm 0)^2 - |\Delta|^2} \sin \alpha}, \\ \hat{g}_2^{R/A} &= \frac{i|\Delta|}{\epsilon \cos \alpha + i\sqrt{(\epsilon \pm 0)^2 - |\Delta|^2} \sin \alpha},\end{aligned}\quad (12)$$

employing the unit matrix 1 and the x component of the Pauli matrix τ_x . The density of states $\rho(\epsilon)$ of surface states is then given by $\rho(\epsilon) = \Im \hat{g}_{11}^R(\epsilon)$. For p -wave superconductor with $\alpha = 0$, $\rho(\epsilon)$ includes mid-gap (ZES):

$$\rho(\epsilon) = \frac{\sqrt{\epsilon^2 - \Delta^2}}{|\epsilon|} \theta(|\epsilon| - \Delta) + \pi \Delta \delta(\epsilon), \quad (13)$$

while for the s -wave case, it includes no ZES , having the well-known BCS form. This difference becomes important when the Kondo effect takes place, because ZES strongly interact with the Kondo resonant state which appears also at $E_F = 0$.

Performing the variation of the effective action with respect to the fields b and λ a couple of self-consistency equations are obtained that determine these fields. In order to explicitly write down these self-consistency equations let us introduce the bare Kondo temperature $T_K^0 = \text{Dexp}[-\pi|\epsilon_0|/(2\Gamma)]$ and define a parameter X by $\Gamma b^2 = T_K^0 X$, where D is the energy bandwidth. Then the MFSBA equations take the form

$$X = -\frac{i\Gamma}{2T_K^0} \text{Tr} \hat{G}^K \tau_z, \quad (14)$$

$$\lambda = \frac{i\Gamma}{8} \text{Tr} [\hat{G}^K \tau_z (\hat{g}_+^R + \hat{g}_+^A) + (\hat{G}^R + \hat{G}^A) \tau_z \hat{g}_+^K] \tau_z, \quad (15)$$

where the trace includes energy integration as well. Eq. (14) effectively determines the Kondo temperature (through the parameter X), and reflects the constraint which prevents double occupancy in the limit $U \rightarrow \infty$. The second self-consistency equation (15) defines the renormalized energy level position $\tilde{\epsilon}$. Let us briefly discuss the validity range of the present analysis.

A comment on the validity of the mean field slave boson approximation scheme and the relation to other approximation schemes is in order. It is known that it gives an adequate description in the Fermi liquid regime of the Kondo effect. (the strong coupling limit.) The Kondo effect is suppressed by Δ as well as by the applied bias voltage eV . If $T_K < \max(\Delta, eV)$, the mean field approximation loses its validity. Fortunately, interesting features appear in the sub-gap voltage regime $eV \leq \Delta$, as we will see below.

Hence the validity of the approximation for the sub-gap region is intimately related with the value of t_K . Quantitatively, our approximation is reliable for sufficiently large t_K . On the other hand, when $t_K < 1$, the Kondo effect is strongly suppressed by superconductivity and consequently we need another approximation scheme such as the non-crossing approximation (NCA) developed in Ref. [18]. This approximation, however, fails to describe the Fermi liquid picture, specified by the region of $t_K \gg 1$. Thus, the mean field approximation constitutes a bridge in calculation methods between the low temperature regime (when the system is a Fermi liquid) and the regime where the NCA is valid.

3 Conductance

The tunneling current I through the quantum dot is given by $I = \langle \hat{I}(t) \rangle$ with

$$\hat{I}(t) = \frac{-ie}{\hbar} \sum_{j\sigma} [\mathcal{T}_j c_\sigma^\dagger b \psi_{j\sigma}(\mathbf{0}, t) - h.c.] \quad (16)$$

and has a simple representation [15] in terms of the dot Green function,

$$I = i \frac{eXt_K}{8\hbar} \text{Tr}[(\hat{G}^R \tau_z - \tau_z \hat{G}^A) \hat{g}_-^K - \hat{G}^K \tilde{g}], \quad (17)$$

where for SKN junctions we denote

$$\tilde{g} = -\gamma_R(\hat{g}^R \tau_z - \tau_z \hat{g}^A) - 2i\gamma_L \tau_z. \quad (18)$$

Being combined with eqs. (14) and (15) the result (17) can be conveniently used for computing the transport current and the differential conductance of an SKN junction in the Kondo regime for different values of t_K and eV/Δ . Here we present the result of our calculations putting special emphasis on the distinction between s -wave and p -wave superconducting leads.

Fig. 1 shows the conductance $G = dI/dV$ and its dependence on V in SKN junctions for both s -wave and p -wave superconducting leads for $t_K = 100, 5, 3$, and 2 with $\Gamma/T_K^0 = 200$. When $t_K = 100$ (the upper curves in Fig.1), the $G - V$ curve shows no difference between s -wave and p -wave superconductors; $G = 4e^2/h$ when $eV < \Delta$ and G decreases gradually when $eV > \Delta$. In this limit, the Kondo resonance reaches the unitary limit, and consequently, this SKN junction reduces to an SN junction with pure ballistic contact, which has already been analyzed [11]. Indeed, in the limit

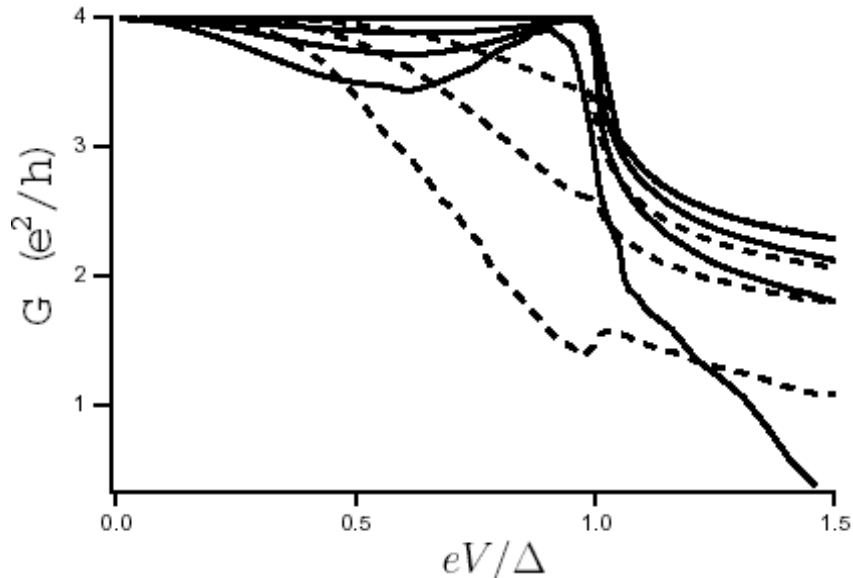


Figure 1: The conductance G (in units of e^2/h) versus the bias V (in units of Δ/e) for an s -wave (dash curves) and p -wave (solid lines) SKN junctions at sub-gap voltages with $\Gamma/T_K^0 = 200$. The parameter t_K takes values 2,3,5,100 (from down up). The upper line corresponding to $t_K = 100$ coincides for s and p wave superconducting leads.

of large $t_K \gg 1$, the expression for the current (16) reduces to that derived in Ref. [11]. For lower values of t_K the distinction between s -wave and p -wave leads becomes prominent.

For s -wave superconductor, as t_K decreases, the Kondo state is driven away from the unitary limit. For $t_K = 5$ the $G-V$ curve noticeably deviates from the one of $t_K = 100$, reflecting the suppression of the Kondo effect due to both Δ and V . For $t_K = 2$ the competition between gap-related suppression of the Kondo effect and the effective transparency of the junction becomes essential, leading to further decrease of the conductance. However, it is interesting to note that for an $S(s\text{-wave})KN$ junction at $t_K = 2$ the conductance displays a small peak at the gap edge. Its interpretation is that the Kondo correlations strongly compete with superconductivity and influence the quasiparticle correlations when the energy exceeds the gap. Such an effect takes place even when $t_K < 1$ (see [18]).

For p -wave superconductor, the $G-V$ curves are less influenced by

variations of t_K in contrast to the situation found for s -wave superconductor, indicating superconductivity plays a minor role in the suppression of the Kondo resonance and the result reported in Ref. [11] persists for smaller values of t_K . The upshot is that ZES support the formation of a Kondo singlet for lower values of t_K , and effectively turn the junction to be more transparent, approaching the unitary limit [11].

4 Shot-noise

The shot-noise power is defined as the symmetrized current-current correlation function

$$K(t_1, t_2) = \hbar[\langle \hat{I}(t_1)\hat{I}(t_2) \rangle - \langle \hat{I} \rangle^2], \quad (19)$$

with the current operator \hat{I} defined in equation (16). The Fourier transform of $K(t_1, t_2)$ gives the shot noise power spectrum $K(\omega)$. The general expression for the zero frequency shot-noise $K(0)$ has been obtained within the mean field slave boson approximation [15]. It is convenient to write it as $K = (K_1 + K_2)e^2\Delta/(8\hbar)$ for which the expressions derived are,

$$K_1 = \frac{Xt_K}{2} \text{Tr}\{(\hat{g}_+^R - \hat{g}_+^A)(\hat{G}^R - \hat{G}^A) - \hat{g}_+^K \hat{G}^K\}, \quad (20)$$

$$K_2 = -\frac{(Xt_K)^2}{8} \text{Tr}\{(\hat{G}^K \tilde{g})^2 - 2\tau_z \tilde{g} \tau_z \hat{G}^A \tilde{g} \hat{G}^R - [2\tilde{g} \hat{G}^R \tau_z \hat{g}_-^K \hat{G}^K - (\hat{G}^A \hat{g}_-^K \tau_z)^2 + \text{h.c.}]\}. \quad (21)$$

Expressions (20) and (21) (supplemented by the self-consistency eqs. (14) and (15)) are then solved numerically for a set of parameters Γ/T_K^0 , t_K .

In Figs. 2 and 3, the zero-energy shot-noise power K and the Fano factor $K/(2eI)$ are displayed versus the applied voltage V for $t_K=100, 5, 3$ and 2 and for $\Gamma/T_K^0=200$. These results are clearly correlated with those for the $G - V$ curve and can be summarized as follows: In the limit $t_K \gg 1$ the characteristics of shot-noise power spectrum for both s -wave and p -wave superconductors are consistent with those obtained for purely ballistic junctions which exhibit strong suppression of the shot-noise power in the sub-gap region. At lower t_K the physics is distinct. For $t_K = 5$ the noise spectrum for s -wave superconducting lead still shows features typical for a junction with relatively high transparency, while the results for $t_K=2$ are

somewhat resemble those for a low transparency junction. Such dependence is explicitly exposed in the plot of the Fano factor versus the applied voltage (see Fig. 3).

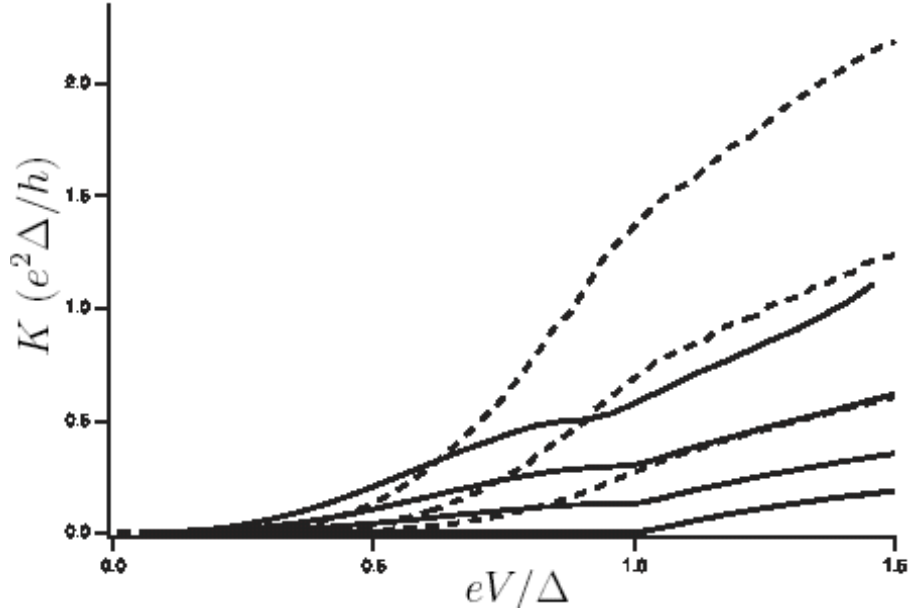


Figure 2: The shot-noise power $K(0)$ (in units of $e^2\Delta/h$) as a function of V (in units of Δ/e) for an SKN junction and for several values of t_K (t_K grows from top to bottom). Dashed (solid) curves correspond to s -wave (p -wave) superconducting lead. The parameters and notations are the same as in Fig. 1. The curves with $t_K=100$ for s and p wave superconductors coincide.

Though the Fano factor does not reach the maximum value of 2, it is strongly enhanced for the smaller value of $t_K = 2$. For p -wave superconductor the shot-noise power (as function of voltage) reflects the same physics as in the conductance: ZES turn the Kondo resonance to be less vulnerable to the impact of superconductivity and the junction remains close to the unitary limit almost in the whole range of values of t_K considered here (see the solid curves on Figs. 2 and 3).

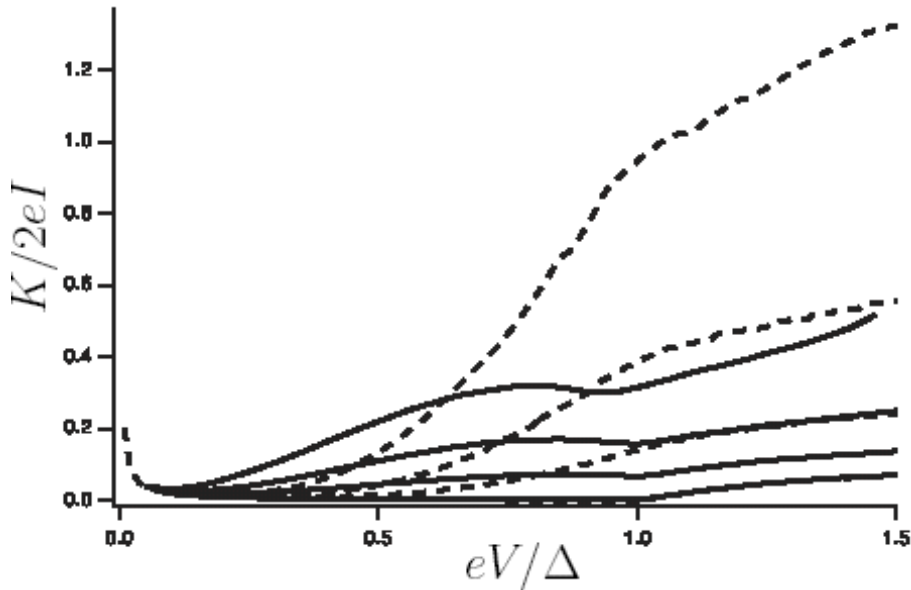


Figure 3: The Fano factor $K/2eI$ as a function of V (in units of Δ/e) for an SKN junction and for several values of t_K (t_K grows from top to bottom). Dashed (solid) curves correspond to s -wave (p -wave) superconducting lead. The parameters and notations are the same as in Fig. 1.

5 Josephson current

In this section we study an equilibrium property (Josephson effect) of an SKS junction in which both electrodes are p -wave superconductors (for comparison we also represent the results for s -wave superconducting leads).

The Free energy F for the Hamiltonian (2) is given by

$$F = -T \sum_{\omega} \ln [\omega^2 (1 + \alpha(\omega))^2 + \tilde{\epsilon}^2 + \beta(\omega)^2 \Delta^2 \cos^2(\delta/2)] + \lambda b^2, \quad (22)$$

with $\alpha(\omega) = \tilde{\Gamma} \sqrt{\omega^2 + \Delta^2} / \omega^2$, $\beta(\omega) = \tilde{\Gamma} / \omega$, $\tilde{\epsilon} = \epsilon + \lambda$, $\tilde{\Gamma} = b^2 \Gamma$ and the phase difference δ between two superconductors. Then the self-consistent equations, $\delta F / \delta \lambda = 0$ and $\delta F / \delta b^2 = 0$ read, respectively

$$\tilde{\epsilon} + \frac{2\Gamma}{\pi} \log \frac{\tilde{\epsilon}}{T_K} = \sum_{\omega} \left[2\Gamma \frac{(1 + \alpha(\omega)) \sqrt{\omega^2 + \Delta^2} + \beta(\omega) \Delta^2 / \omega \cos^2 \frac{\delta}{2}}{(1 + \alpha(\omega))^2 \omega^2 + \tilde{\epsilon}^2 + \beta(\omega)^2 \Delta^2 \cos^2 \frac{\delta}{2}} - \frac{2\Gamma |\omega|}{\omega^2 + \tilde{\epsilon}^2} \right], \quad (23)$$

$$\tilde{\Gamma} = \Gamma \sum \left[\frac{2\tilde{\epsilon}}{(1 + \alpha(\omega))^2 \omega^2 + \tilde{\epsilon}^2 + \beta(\omega)^2 \Delta^2 \cos^2 \frac{\delta}{2}} \right]. \quad (24)$$

Self consistent equations for the case of *s*-wave superconducting leads were derived in Ref. [19].

The Josephson current is given by, $I = (2e/\hbar)\partial F/\partial\delta$, that is,

$$I = \frac{e}{\hbar} \sum_{\omega} \frac{(\beta(\omega)\Delta)^2 \sin \delta}{\omega^2(1 + \alpha(\omega))^2 + \tilde{\epsilon}^2 + (\beta(\omega)\Delta)^2 \cos^2 \frac{\delta}{2}}. \quad (25)$$

The self-consistency equation and the expression for the Josephson current can easily be extended to the case of an anisotropic coupling: $\Gamma_{L/R} = \Gamma(1 \pm p)$ (the anisotropy parameter $0 < p < 1$). For this, one should replace $\cos^2 \frac{\delta}{2} \rightarrow (\cos^2 \frac{\delta}{2} + p^2 \sin^2 \frac{\delta}{2})$ and $I \propto \sin \delta \rightarrow I \propto (1 - p^2) \sin \delta$.

In the unitary limit $T_K \gg \Delta$, $\tilde{\epsilon} = 0$ we can approximate

$$\alpha(\omega) = \tilde{\Gamma} \sqrt{\omega^2 + \Delta^2/\omega^2} \gg 1$$

since the relevant energy scale for the superconductor is $\omega \leq \Delta$. As a result, the Josephson current (25) for *p*-wave superconductor is

$$J = \frac{2e\Delta}{\hbar} \frac{(1 - p^2)}{4} \frac{\tanh(\beta\Delta f(\delta)/2)}{f(\delta)} \sin \delta \quad (26)$$

with $f(\delta) = \sqrt{1 + \cos^2(\delta/2) + p^2 \sin^2(\delta/2)}$, which is different from the one for *s*-wave [23].

In Fig. 4, the Josephson current is calculated as a function of the phase difference δ for a small anisotropy parameter $p = 0.1$ and for values of $t_K = 100, 5, 3$, and 2 at temperatures close to $T = 0$.

For an *s*-wave superconductor (dashed lines in Fig. 4) the current at $t_K = 100$ is nearly the same as the one at the unitary limit [23]; It deviates from the sinusoidal form and reaches its maximum around $\delta = \pi$. At lower values of t_K , the current characteristic is similar but its amplitude is suppressed. Nevertheless, in this region of parameters, the Kondo effect overcomes superconductivity and the impurity spin is screened. Hence there are no traces of a π -junction.

For *p*-wave superconductor (solid lines in Fig. 4), the current at $t_K = 100$ is approximately given by Eq. (26), which is qualitatively different from that obtained for the *s*-wave superconductor; The current has its maximal value around $\pi/2$ and the curve is very close to being sinusoidal. This result is very similar to the one encountered in *SIS* junctions. The mid-gap states act as

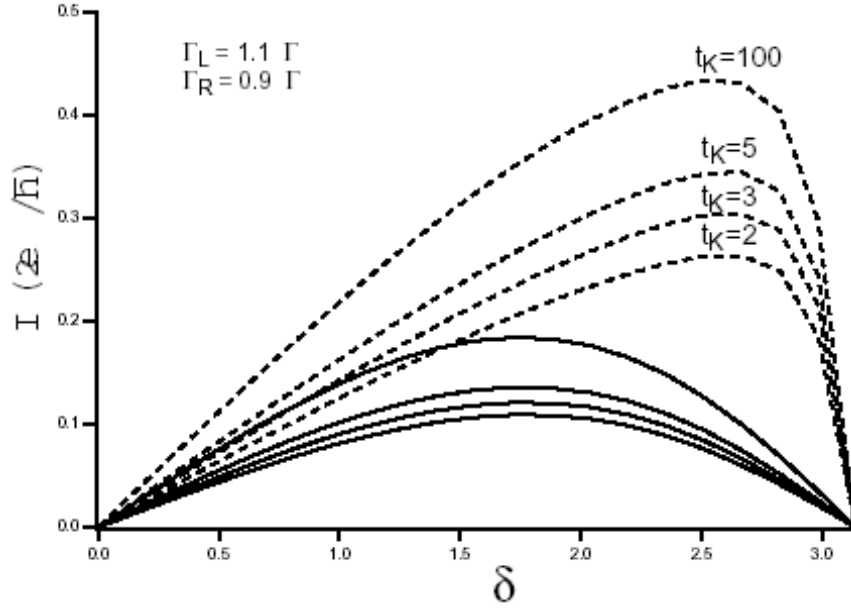


Figure 4: Josephson current versus phase difference δ at $T \rightarrow 0$. Dash and solid curves correspond to s and p -wave superconductors, respectively. The parameters are the same as in Fig.1. The value of t_K decreases from top downward.

if they increase the effective normal region of the junction and therefore, the junction becomes more resistive, which makes the contact of the junction less transparent, again in marked distinction from the s -wave case. Indeed, the amplitude of the Josephson current is reduced compared with its value for the s -wave junction.

Similar analysis holds for the temperature dependence of the Josephson current. Fig. 5 displays the maximum Josephson current $I(T)$ as function of temperature for s -wave (dashed lines) and p -wave (solid lines) superconducting leads. For p -wave junctions, $I(T)$ assumes relatively large values near $T = T_C$ while for s -wave junctions, it decreases more rapidly as T increases. The difference is more prominent when t_K becomes smaller. These results are explained by the same reasoning above; the temperature dependence is more similar to the usual SIS junction for the p -wave case, while for s -wave superconductors it is closer to the one in SNS junctions. This difference stems from the existence of ZES. The situation is similar to the

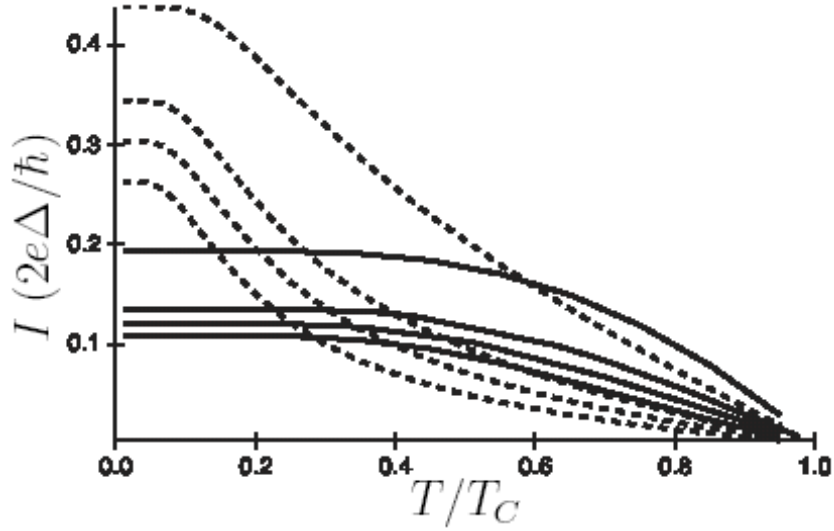


Figure 5: Temperature dependence of the maximum Josephson current for s -wave (dashed curves) and p -wave (solid curves) superconducting leads for $t_K = 100, 5, 3$ and 2 (from top to bottom). The phase δ of each curve is chosen so as to give the maximum value of Josephson current at $T = 0$ in Fig. 4. Other parameters are the same as in Fig. 1.

one encountered in Josephson current through an SIS system [24].

In conclusion, we have analyzed an important physical problem involving strong correlations, the Kondo effect and unconventional superconductivity in the regime $T < \Delta < T_K$. These aspects can be realized in an SKN junction consisting of an Anderson impurity in the Kondo regime. The S electrode consists of a p -wave superconductor specially oriented with respect to the contact surface allowing the formation of zero energy bound-states in the middle of the gap. First, we have investigated non-equilibrium aspects and elucidated the nonlinear $G - V$ characteristics. Moreover, we calculated the shot-noise power spectrum of SKN junctions at voltages $eV \leq \Delta$. It is found that at sufficiently large t_K the Kondo resonance effectively turns the junction behavior to be similar to that of highly transparent non-interacting weak links for both s and p -wave superconductors. However, when the ratio of the Kondo temperature to the superconducting gap becomes smaller the behavior of these two types of junctions is quite different: the Kondo resonance persists much more effectively for junctions with p -wave leads than it does for s -wave leads. Similar effects emerge also in the (equilibrium)

Josephson current which has also been calculated above.

We would like to thank Y. Tanaka for very helpful and stimulating discussions. This research is supported by DIP German Israel Cooperation project *Quantum electronics in low dimensions* by the Israeli Science Foundation grant *Many-Body effects in non-linear tunneling* and by the US-Israel BSF grant *Dynamical instabilities in quantum dots*. One of us (TA) is supported by JSPS Research Fellowships for Young Scientists.

References

- [1] Y. Maeno, H. Hashimoto, K. Yoshida, S. Nishizaki, T. Fujita, J.G. Bednorz, and F. Lichtenberg, *Nature* **372**, 532 (1994).
- [2] A.C. Hewson, *The Kondo Problem to Heavy Fermions* (Cambridge University Press, Cambridge, 1993).
- [3] L.I. Glazman and M.E. Raikh, *Pis'ma Zh. Eksp. Teor. Fiz.* **47**, 378 (1988) [*JETP Lett.* **47** 452 (1988)]; T. K. Ng and P.A. Lee, *Phys. Rev. Lett.* **61**, 1768 (1988).
- [4] S. Hershfield, J.H. Davies, and J.W. Wilkins, *Phys. Rev. Lett.* **67**, 3720 (1991).
- [5] Y. Meir, N.S. Wingreen, and P.A. Lee, *Phys. Rev. Lett.* **70**, 2601 (1993).
- [6] D. Goldhaber-Gordon, H. Shtrikman, D. Mahalu, D. Abusch-Magder, U. Meirav, and M.A. Kastner, *Nature* **391**, 156 (1998); S.M. Cronenwett, T.H. Oosterkamp and L.P. Kouwenhoven, *Science* **281**, 540 (1998); J. Schmid, J. Weis, K. Eberl and K. v. Klitzing, *Physica B*, **256**, 182 (1998); F. Simmel, R.H. Blick, J.P. Kotthaus, W. Wegscheider, and M. Bichler, *Phys. Rev. Lett.* **83**, 804 (1999).
- [7] M.A. Kastner, *Comm. Cond. Matt.* **17**, 349 (1996).
- [8] J. Nygard, D.H. Cobben, and D.E. Lindelof, *Nature* **408**, 342 (2000).
- [9] W.G. van der Wiel, S. De Franceschi, T. Fujisawa, J.M. Elzerman, S. Tarucha, and L.P. Kouwenhoven, *Science* **289**, 2105 (2000).
- [10] G.A. Fiete, J.S. Hersch, E.J. Heller, H.C. Manoharan, C.P. Lutz, and D.M. Eigler, *Phys. Rev. Lett.* **86**, 2392 (2001); M.A. Schneider, L. Vitali, N. Knorr, and K. Kern, *Phys. Rev. B* **65**, 121406

- (2002); J. Park, A.N. Pasupathy, J.I. Goldsmith, C. Chang, Y. Yaish, J.R. Petta, M. Rinkoski, J.P. Sethna, H.D. Abruña, P.L. McEuen, and D.C. Ralph, *Nature* **417**, 722 (2002); W. Liang, M.P. Shores, M. Bockrath, J.R. Long, and H. Park, *Nature* **417**, 725 (2002).
- [11] T.M. Klapwijk, G.E. Blonder, and M. Tinkham, *Physica B* **109-110**, 1157 (1982).
- [12] A.Yu. Kasumov, R. Deblock, M. Kociak, B. Reulet, H. Bouchiat, I.I. Khodos, Yu.B. Gorbatov, V.T. Volkov, C. Journet, and M. Burghard, *Science* **284**, 1508 (1999).
- [13] M.R. Buitelaar, T. Nussbaumer, and C. Schönberger, *Phys. Rev. Lett.* **89**, 256801 (2002).
- [14] Y. Avishai, A. Golub, and A.D. Zaikin, *Phys. Rev. B* **63**, 134515 (2001); *Europhys. Lett.* **54**, 640 (2001).
- [15] Y. Avishai, A. Golub, and A.D. Zaikin, *Phys. Rev. B* **67**, 041301 (2003).
- [16] R. Fazio and R. Raimondi, *Phys. Rev. Lett.* **80**, 2913 (1998); **82**, 4950 (E)(1999).
- [17] P. Schwab and R. Raimondi, *Phys. Rev. B* **59**, 1637 (1999).
- [18] A.A. Clerk, V. Ambegaokar, and S. Hershfield, *Phys. Rev. B* **61**, 3555 (2000).
- [19] A.V. Rozhkov and D.P. Arovas, *Phys. Rev. B* **62**, 6687 (2000).
- [20] G. Campagnano, D. Giuliano, and A. Tagliacozzo, *cond-mat/0106532* (2001).
- [21] Y. Tanaka, T. Hirai, K. Kusakabe, and S. Kashiwaya, *Phys. Rev. B* **60**, 6308 (1999).
- [22] P. Coleman, *Phys. Rev. B* **29**, 3035 (1984).
- [23] L. Glazman and K.A. Matveev, *Pis'ma Zh. Eksp. Teor. Fiz.* **49**, 570 (1989) [*JETP Lett.* **49**, 659 (1989)].
- [24] Y. Tanaka, and S. Kashiwaya, *Phys. Rev. B* **56**, 892 (1997); S. Kashiwaya, and Y. Tanaka, *Rep. Prog. Phys.* **63**, 1641 (2000).